

Multipole Analysis of the Electron Density in Triphylite, LiFePO_4 , using X-ray Diffraction Data

BY VICTOR A. STRELTSOV*

Institute of Crystallography, Russian Academy of Sciences, Leninsky pr. 59, Moscow 117333, Russia

ELENA L. BELOKONEVA

Department of Crystallography and Crystal Chemistry, Moscow State University, Leninskiye Gory, Moscow 119899, Russia

VLADIMIR G. TSIRELSON

Department of Physics, Mendeleev Institute of Chemical Technology, Miusskaya sq. 9, Moscow 125820, Russia

AND NIELS K. HANSEN

Laboratoire de Mineralogie, Cristallographie et Physique Infrarouge, URA-CNRS 809, Universite de Nancy I, BP 239, F-54506 Vandoeuvre les Nancy CEDEX, France

(Received 9 December 1991; accepted 27 April 1992)

Abstract

The electron density distribution and 3d-orbital electron occupancies for the Fe atom in synthetic triphylite, LiFePO_4 , have been analysed using single-crystal X-ray diffraction data measured at $T = 298$ K with $\text{Mo } K\alpha$ ($\lambda = 0.71069$ Å) radiation to a resolution corresponding to $(\sin\theta_{\text{max}}/\lambda) = 1.078$ Å⁻¹. Measurements of 3265 reflections gave 944 unique data [$R_{\text{int}}(I) = 0.036$] with $I > 2\sigma(I)$. For an atomic multipole density model fitted by least-squares methods $R(F) = 0.0174$ for all unique reflections. The Fe atom 3d-orbital occupancies have been derived from the multipole population coefficients using point-group-specific relations. The asphericity of the electron deformation density around the Fe atom is discussed using crystal-field theory and magnetic properties of triphylite. Crystal data: lithium iron(II) phosphate, LiFePO_4 , $M_r = 157.76$, orthorhombic, $Pnma$, $a = 10.332$ (4), $b = 6.010$ (5), $c = 4.692$ (2) Å, $V = 291.4$ (3) Å³, $Z = 4$, $D_x = 3.596$ Mg m⁻³, $\mu = 5.65$ mm⁻¹, $F(000) = 304$.

Introduction

The crystal structure of LiFePO_4 , which has been studied by Yakubovich, Simonov & Belov (1977) and described in more detail by Yakubovich, Belokoneva, Tsirelson & Urusov (1990), has an olivine-type structure with a distorted hexagonal

* Author to whom correspondence should be addressed. Present address: Crystallography Centre, University of Western Australia, Nedlands, Western Australia 6009, Australia.

anion close packing, where the cations occupy three different positions: a tetrahedral (P) site and two octahedral sites. An ORTEP (Johnson, 1965) plot showing the cation coordination is given in Fig. 1. One octahedral site lies at the inversion centre and the other is in the mirror plane. As usual in olivine-type structures the former octahedral site is occupied by cations with smaller charge (Li) and the latter by cations with larger charge (Fe). The main feature of the LiFePO_4 crystal structure consists of olivine-type ribbons extending along the b crystal axis. The Li octahedra protrude from the olivine ribbon and are connected along their edges and with the larger Fe

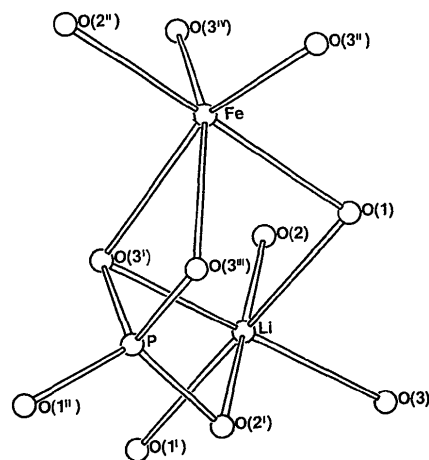


Fig. 1. ORTEP view (Johnson, 1965) of the coordination close to cations. The c axis is directed approximately across the figure.

octahedra. PO₄ tetrahedra have three of the six edges in common with the cation octahedra. These edges have the shortest lengths and differ significantly from the other O—O distances.

The magnetic structure of LiFePO₄ has been determined by Santoro & Newnham (1967) from neutron diffraction data. Below the Néel temperature $T_N = 50$ K, the spin vectors associated with these Fe-atom positions are antiparallel and align in an antiferromagnetic array collinear with the *b* axis. The magnetic space group is P_{nma} . As has been shown (Santoro & Newnham, 1967), the only Fe—O—Fe superexchange interactions give rise to antiferromagnetic puckered planes orthogonal to *a*. There are no direct or superexchange linkages between these planes, and long-range interactions, such as Fe—O—P—O—Fe triple exchange, have been suggested.

The present paper describes a study of the electron deformation density in synthetic crystalline triphylite, LiFePO₄. A multipole refinement of the X-ray diffraction data has been carried out using different approximations for the site symmetry of the Fe atoms. Values of 3*d*-orbital occupancies for the Fe atom were calculated from the results of multipole charge-density model refinement. The relations between the electron density distribution and the magnetic properties have been discussed.

Experimental

Isometric transparent pink-coloured crystals of triphylite were grown by hydrothermal synthesis at the Institute of Crystallography, the Russian Academy of Sciences, as described by Belov, Ivaschenko & Matvienko (1981). A spherical ground crystal with radius $r = 0.125$ mm was used for accurate X-ray diffraction measurements. Intensities of 3265 reflections (up to $\sin\theta/\lambda = 1.078 \text{ \AA}^{-1}$, $2\theta_{\max} = 100^\circ$) over one half of the sphere $0 \leq h \leq 18$, $-12 \leq k \leq 12$ and $-10 \leq l \leq 10$ (four equivalents per general reflection) were measured with an automatic four-circle Syntex $P\bar{1}$ diffractometer using monochromatized (graphite) Mo $K\alpha$ radiation. The unit-cell dimensions were determined from 15 reflections with 2θ values between 41 and 50° . Every reflection profile was step-scanned in $\omega/2\theta$ mode with the scan rate variable from 2 to $24^\circ \text{ min}^{-1}$. The scan-width parameter was $(2 + 0.8 \tan\theta)^\circ$. Diffractometer stability was checked by periodic measurement of a standard reflection (311) variation. Maximum intensity variation of the standard was 2%. After analysis of equivalents, 135 high-angle reflections differed significantly from the averaged equivalents (greater than 18%) and were ignored. The internal-agreement index, defined as $R_{\text{int}} = \sum |I - \langle I \rangle| / \sum I$, was 0.036. The final experimental data consisted of 944 unique reflections with $I > 2\sigma(I)$.

Refinement

Conventional least-squares refinement

Initially, the experimental data were corrected for absorption ($\mu r = 0.7$) using the *MINEXTL* package (Gerr *et al.*, 1991). The transmission range was 0.36 to 0.40. Lorentz and polarization corrections were applied. The refinement was by a full-matrix least-squares procedure using an anisotropic approximation for the thermal parameters and a Zachariasen isotropic extinction correction (Larson, 1970) based on $|F_o|$ with weights $w = 1/\sigma^2(F_o)$. The starting structural parameters were taken from Yakubovich, Belokoneva, Tsirelson & Urusov (1990). The refinement converged to $R(F) = 0.023$ and $wR(F) = 0.030$ with the lowest extinction correction $y_{\min} = 0.81$ for the 020 reflection (the observed structure factor $F_{\text{obs}} = y_{\min} F_{\text{kin}}$, where F_{kin} is the kinematical value of the structure factor). In order to minimize the influence of aspherical distortion of the atomic electron density on the positional and thermal parameters the refinement of those 40 parameters with the scale factor was carried out using 672 high-angle reflections with $(\sin\theta/\lambda > 0.6 \text{ \AA}^{-1})$. The final agreement indices were $R(F) = 0.020$, $wR(F) = 0.026$, $\text{GoF} = 3.71$ and $\text{max. shift/e.s.d.} = 0.00044$. Structural parameters and interatomic distances are listed in Tables 1 and 2.*

Multipole charge-density model refinement

The structural parameters obtained for the high-angle refinement were used in a multipole refinement carried out with the program *MOLLY* (Hansen & Coppens, 1978; Hansen, 1991) adapted for an IBM PC computer. The refinable parameters were the scale factor, the valence-shell contraction–expansion parameters k and k' (Coppens, Guru Row, Leung, Stevens, Becker, & Yang, 1979) and the multipole population parameters P_{val} and P_{lm} . The limit $l_{\max} = 4$ was used for truncation of the multipole expansion at the hexadecapole level. The radial functions were $r^{n_l} \exp(-k' \zeta r)$ with $n_l = 4, 4, 6, 8$ (*P*) and $n_l = 2, 2, 3, 4$ (*O*) for $l = 1, 2, 3, 4$ and $n_l = 4$ for all these l values (Fe). Initial values of the orbital exponent coefficient ζ were from Clementi & Raimondi (1963). All core, valence, isolated-atom and Li⁺-cation scattering factors with anomalous dispersion were taken from *International Tables for X-ray Crystallography* (1974, Vol. IV).

Several constraints were imposed on the multipole refinement: the total-valence population correspon-

* Lists of structure factors, anisotropic thermal and multipole parameters, and figures for static deformation density have been deposited with the British Library Document Supply Centre as Supplementary Publication No. SUP 55228 (12 pp.). Copies may be obtained through The Technical Editor, International Union of Crystallography, 5 Abbey Square, Chester CH1 2HU, England. [CIF reference: AS0589]

Table 1. Fractional coordinates ($\times 10^5$), U_{eq} values ($\text{\AA}^2 \times 10^5$) and site symmetry of atoms in LiFePO_4

$$U_{eq} = (1/3)\sum_i \sum_j a_i^* a_j^* \mathbf{a}_i \cdot \mathbf{a}_j.$$

	x	y	z	U_{eq}	Crystallographic	Local (assumed)
Li	0	0	0	1700 (100)	$\bar{1}$	—
Fe	28222 (3)	$\frac{1}{4}$	97472 (6)	624 (5)	m	$m3m^a$ or m^b
P	09486 (5)	$\frac{1}{4}$	41820 (10)	507 (9)	m	$mm2$
O(1)	09678 (15)	$\frac{1}{4}$	74279 (29)	820 (30)	m	m
O(2)	45710 (14)	$\frac{1}{4}$	20602 (29)	780 (30)	m	m
O(3)	16558 (10)	4646 (16)	28478 (21)	810 (20)	1	m

Notes: (a) model (I), (b) model (II).

Table 2. Interatomic distances (\AA)

Fe octahedron		Li octahedron		P tetrahedron	
Fe—O(1)	2.204 (2)	Li—O(1) ⁱⁱⁱ	2.171 (1) [2]	P—O(1 ⁱⁱ)	1.524 (2)
—O(2) ^{iv}	2.108 (2)	—O(2) ^v	2.087 (1) [2]	—O(2) ^v	1.538 (2)
—O(3) ^v	2.251 (1) [2]	—O(3)	2.189 (1) [2]	—O(3 ⁱ)	1.556 (1) [2]
—O(3 ⁱⁱ)	2.064 (2) [2]				

Symmetry code: (i) $x, y, z + 1$; (ii) $\frac{1}{2} - x, -y, \frac{1}{2} + z$; (iii) $x, y, z - 1$; (iv) $\frac{1}{2} - x, -y, -\frac{1}{2} + z$; (v) $-\frac{1}{2} + x, \frac{1}{2} - x, \frac{1}{2} - z$.

Table 3. Least-squares refinement statistics of fit

Model	(I)	(II)	(III)
Fe-site symmetry	$m3m$	m	m
Extinction	Type II	Type II	Type I
R	0.0187	0.0174	0.0176
wR	0.0303	0.0290	0.0295
S	1.901	1.828	1.864
χ^2	3158	2882	2998
n^a	944	944	944
m^b	70	81	81
$F_{b,n-m}$		7.50	34.7
$F_{b,n-m,\alpha}$ ($\alpha = 0,05$) ^c		1.87	3.9

Notes: (a) the number of reflections, (b) the number of parameters, (c) the critical point of F distribution.

ded to an electrically neutral unit cell; the valence population of the Li cation was fixed at $P_{\text{val}} = 0$ and the electron deformation density of Li was not refined. In order to reduce the number of variable parameters, chemical symmetry was imposed on the multipole model for atomic electron densities. The crystallographic and site symmetry of the atoms assumed in triphylite are given in Table 1. The index-picking rules for site-symmetry spherical harmonics were taken from Kurki-Suonio (1977).

The phosphorus deformation was described by approximately tetrahedral $mm2$ local symmetry with the twofold axis parallel to the local Cartesian z axis [the local x axis was parallel to the O(1ⁱⁱ)—O(2^v) line and the y axis was parallel to the O(3ⁱ)—O(3ⁱⁱⁱ) line (Fig. 1)]. All oxygen atoms O(1), O(2) and O(3) had identical m deformation symmetry, with the local z axis perpendicular to the m plane which was defined by two P—O vectors for each O atom. The local x axes of Cartesian systems for O atoms were along the P—O bonds and y axes were in the m planes.

Two different descriptions of deformation were used for the Fe atom. Although in triphylite the Fe atoms occupy holes in distorted hexagonal oxygen

close packing, an attempt was made to refine multipole population parameters under the constraint of perfect octahedral $m3m$ symmetry, with one trigonal axis parallel to the crystallographic c axis. Only two multipole functions are allowed for $l_{\text{max}} = 4$ in a coordinate system with a threefold axis parallel to the [111] direction. These are a monopole, and the cubic harmonic $(x^4 + y^4 + z^4)/r^4 - 3/5$, which is a combination of y_{40} and y_{44+} functions. By refining the corresponding population parameters (P_{40} and P_{44+}) independently a tetragonal distortion of the octahedral symmetry was allowed for. Least-squares statistical descriptors for this refinement (model I) are given in Table 3. Another multipole refinement was carried out taking into account only the crystallographic mirror plane m (model II). In this case the local coordinate system for the Fe atom corresponds to the crystallographic system (the local x and z axes are parallel to the crystal a and c axes and lie in the m plane; the local y axis is parallel to the crystal b axis and perpendicular to the m plane). A statistical F test indicates that lowering the symmetry (*i.e.* increasing the number of parameters refined) significantly improves the fit to the experimental data. The resulting multipole populations are useful practically according to the analysis of Draper & Smith (1981), because the calculated $F_{b,n-m}$ value is at least four times greater than the $F_{b,n-m,0.05}$ table value (columns I and II in Table 3). We will therefore only discuss the model with crystallographic symmetry at the Fe site. In the final refinement the 81 parameters for model (II) were optimized using all unique reflections with a weighting scheme $w = 1/[\sigma^2(F) + 0.0002F^2]$ which was chosen on the basis of the analysis of the δR curve of Abrahams & Keve (1971). The refined parameters include the scale factor and an isotropic type-II extinction parameter (Becker & Coppens, 1974). The lowest extinction correction coefficient was $y_{\text{min}} = 0.80$ for the 020 reflection. A multipole model with an isotropic type-I (Gaussian distribution function) extinction parameter was also refined. The result is presented in the third column of Table 3 ($y_{\text{min}} = 0.74$ for the 020 reflection). But the statistical data in Table 3 ($F_{b,n-m} \gg F_{b,n-m,\alpha}$) indicates that the model with the type-II extinction parameter is preferable for the

triphylite crystal studied. The final multipole model (II) (extinction type II) parameters are deposited.* Including a $4s$ density function for the Fe atom in the model hardly modified these results. The same behaviour has been observed for Fe atoms in other crystals as noted by Holladay, Leung & Coppens (1983), Tsirelson, Streltsov, Ozerov & Ivon (1989) and Streltsov, Tsirelson & Ozerov (1990).

Electron density maps

Electron deformation density distribution

The electron deformation density calculation included all unique reflections up to $\sin\theta/\lambda = 0.75 \text{ \AA}^{-1}$. Addition of the high-angle reflections in the summation resulted only in ripples in the electron density maps due to the rather noisy experimental structure factors at high angles. The average random error of the total electron density corresponding to the resolution of the presented maps is estimated as $0.02 e \text{ \AA}^{-3}$.

The deformation density maps in different sections of the PO₄ tetrahedron are displayed in Fig. 2. The main feature of the deformation density in the section through the tetrahedron face with the shortest edges (Fig. 2*a*) is polarization of the electron density for O atoms mainly along the olivine ribbon parallel to b crystal axis. The deformation density in the sections containing the P atom is shown in Figs. 2(*b*) and 2(*c*). The positive deformation density peaks shift from the P—O(2) and P—O(3) lines in the direction of the P—O(1) line. This may be explained by the strain of the P—O(2) and P—O(3) bonds because the angles O(1)—P—O(2) [112.97 (8)°] and O(1)—P—O(3) [113.37 (5)°] involving the O(1) atom are larger than the others: O(2)—P—O(3) [106.41 (5)°] and O(3)—P—O(3) [103.54 (7)°]. The electron density distribution near the P atom may be approximated by an sp^3 -hybridization electron state. Lone-pair density features observed near the O atoms are very delocalized. In general the deformation density for the phosphate group of triphylite is in close agreement with that obtained by Hansen, Protas & Marnier (1991) for KTiOPO₄. Values of the positive deformation density in the bonds are close to those of the theoretical calculation of the deformation density in H₃PO₄ (Blessing, 1988).

Our major interest is in the deformation density distribution around the Fe atom. Figs. 3(*a*) and 3(*b*), which show deformation density maps in the (001) and (010) sections of the unit cell, contain six positive peaks near the atom [four high peaks in the (001) plane in Fig. 3*a* and two low peaks along the c axis in Fig. 3*b*]. According to crystal-field theory the crystal environment with mirror-plane symmetry m

splits the $3d$ -orbital fivefold degenerate level into five differently occupied orbitals. Using the local coordinate system from Table 1, the four positive peaks in

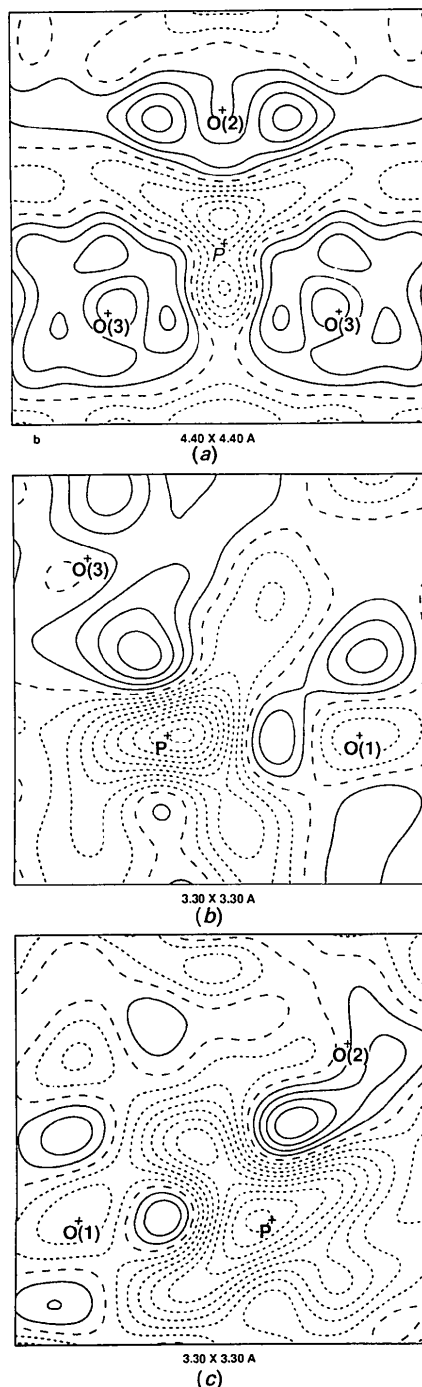


Fig. 2. Electron deformation density maps in the planes of (a) O(2)—O(3)—O(3) (the b axis is directed across the figure), (b) P—O(1)—O(3) and (c) P—O(1)—O(2). Interval between contours $0.1 e \text{ \AA}^{-3}$ with continuous contours for positive density, broken for zero and dashed for negative. The atoms located out of the plane are labeled with an italic font.

* See deposition footnote.

Fig. 3(a) may reflect a preferential population of the $d_{x^2-y^2}$ orbital, and the two weaker positive features in Fig. 3(b) of the d_{z^2} orbital. We can compare our deformation density around the Fe atom with results for the olivine structure fayalite (α -Fe₂SiO₄) (Fujino, Sasaki, Takeuchi & Sadanaga, 1981). In fayalite a set of positive peaks having absolute heights greater than $0.6 \text{ e } \text{Å}^{-3}$ were observed in the (001) plane near the Fe-atom position with m symmetry.

The map containing four O(3) atoms in the Fe octahedron is shown in Fig. 3(c). The Fe atom is located 0.1 Å out of the plane. Fig. 3(c) shows a polarization of the deformation density of the O atoms towards the position of the Fe atom as a result of metal-ligand bonding in which the d_{xy} , d_{xz} and d_{yz} orbitals of the Fe atoms are possibly involved. In addition, the section in Fig. 3(d) through the two nearest Fe atoms (the Fe-Fe distance is 3.87 Å and the crystallographic positions are $x, \frac{1}{4}, z$ and $\bar{x} + \frac{1}{2}, \frac{3}{4}, z + \frac{1}{2}$) and the O(3) atom [O(1) is 0.04 Å out of the plane] shows the same tendency to linkage between the Fe atoms and the close ligating oxygens. These

atoms take part in an Fe—O—Fe superexchange interaction below the Néel temperature. The positive deformation peak between the Fe atom and the O(1) atom in Figs. 3(b) and 2(c) (the peak in the bottom left corner) connects the Fe atom with the PO₄ tetrahedron in the a direction; this correlates with the possibility of long-range Fe—O—P—Fe triple exchange between antiferromagnetic puckered planes orthogonal to a (Santoro & Newnham, 1967).

The deformation density distribution in the LiO₆ octahedra indicates a large electron shift towards the O atoms, in agreement with the usual models of ionic bonding, and is not presented here.

Maps of static model deformation electron density for triphylite were computed by the program *SALLY* (Hansen, 1991) using the cluster of atoms presented in Fig. 1. Two different sections corresponding to the crystallographic deformation density maps in Figs. 2(c) and 3(a) have been deposited.* The crystallographic and model deformation densities agree well.

* See deposition footnote.

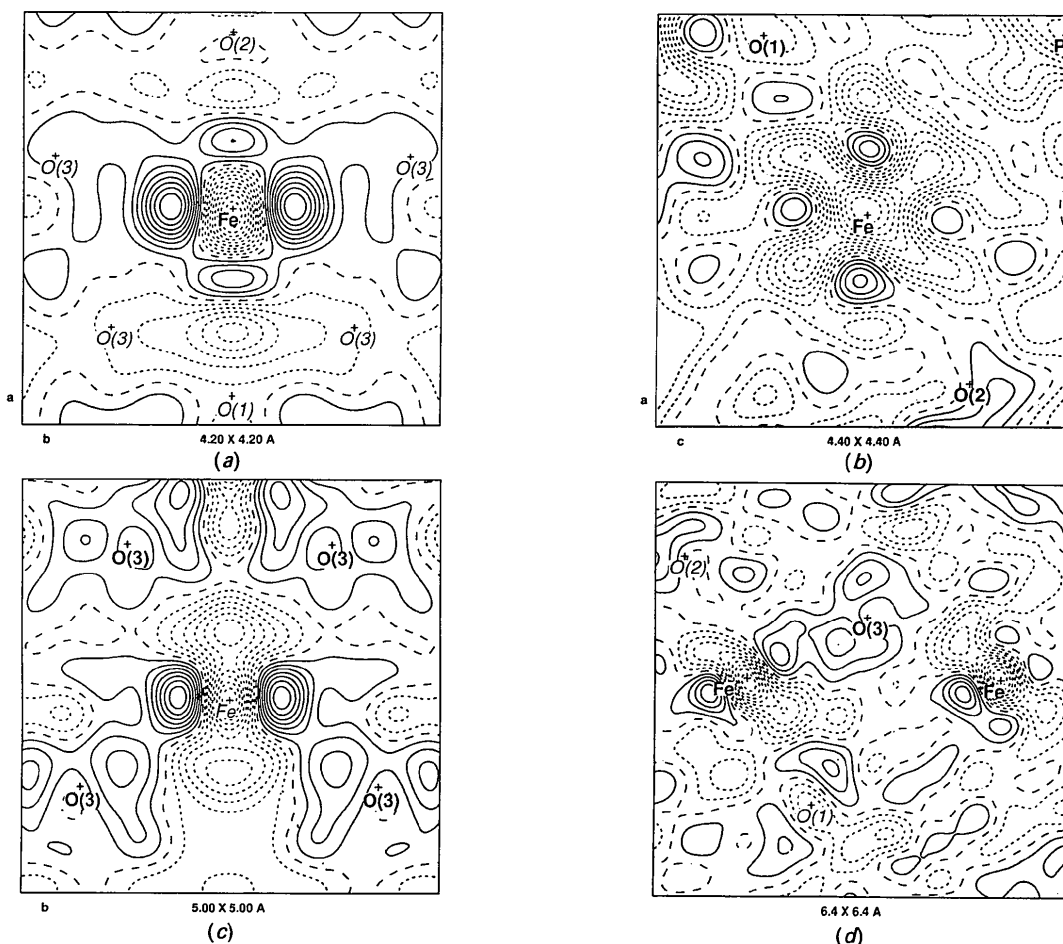


Fig. 3. Electron deformation density maps containing the Fe atom in the planes of (a) (001) and (b) (010). Map (c) in the plane through four O(3) atoms of the Fe octahedron and (d) in the plane through Fe—O(3)—Fe atoms. Contours and labels as in Fig. 2.

Table 4. *Orbital population for the Fe atom in LiFePO₄*

	Multipole refinement	Natural orbitals		Spherical atom	
d_{z^2}	1.81 (9)	1.95 (9)	29.3%	1.2	20.0%
$d_{x^2-y^2}$	2.13 (13)	2.15 (12)	32.4%	1.2	20.0%
d_{xy}	0.77 (13)	0.73 (13)	11.0%	1.2	20.0%
d_{xz}	0.77 (8)	0.61 (8)	9.2%	1.2	20.0%
d_{yz}	1.16 (8)	1.20 (5)	18.1%	1.2	20.0%
Σd	6.64 (23)	6.64 (23)		6.0	
$d_{z^2/xz}$	0.40 (2)				
d_{z^2/x^2-y^2}	0.08 (1)				
d_{xz/x^2-y^2}	-0.17 (1)				
$d_{yz/xy}$	-0.13 (1)				

3d-orbital occupancies of the Fe atom

The expressions relating multipole population parameters to d -orbital occupancies for transition-metal atoms have been derived by Holladay, Leung & Coppens (1983). On the basis of these relations the 3d-orbital occupancies of the Fe atom in triphylite were determined. The electron population of the five 3d orbitals of the Fe atom in the m symmetry crystal field are presented in Table 4. The d orbitals in this point group belong to either (a) d_{z^2} , $d_{x^2-y^2}$ and d_{xy} or (b) d_{xz} and d_{yz} representations. The cross terms $d_i d_j$ (Holladay, Leung & Coppens, 1983) which are symmetry allowed for the Fe-atom position in triphylite are presented as well.

In order to determine the natural orbital populations the 5×5 population matrix was diagonalized and corresponding values of the populations are listed in Table 4. We also transformed the d -orbital populations to a coordinate system related to the close-ligating O atoms: x and y axes parallel to the plane of the four O(3) atoms, and thus z parallel to the O(1)—O(2) direction. The cross terms obtained were larger than in Table 4, that is the d -orbitals of Fe in triphylite are indeed closely related to the crystal axes.

The analysis of the 3d-orbital occupancies of the Fe atom indicates the electron population of the d_{z^2} and $d_{x^2-y^2}$ orbitals is higher in comparison with the spherically averaged free atom and that the d_{z^2} orbital is slightly depopulated relative to the $d_{x^2-y^2}$ orbital which has population larger than 2. The unphysical value can be explained by fairly large overlap between the Fe and O atomic orbitals in the xy plane while the expression relating d -orbital occupancies to multipole parameters (Holladay, Leung & Coppens, 1983) is valid under the assumption that the overlap between metal atom and ligand orbitals is small.

Atomic charges

The net charges of the atoms in LiFePO₄ from the refined monopole population parameters were determined: Li = +1 (not refined), Fe = +1.35 (16),

P = +0.77 (40), O(1) = -0.83 (14), O(2) = -0.81 (14), O3 = -0.74 (11). The net charge of the Fe atom in triphylite is very close to that in fayalite [+1.54 (7)] obtained by Fujino, Sasaki, Takeuchi & Sadanaga (1981) from direct integration of the electron density within the sphere of a nearly defined radius around the cation. The net charge of the phosphate group is -2.35 (21). It should be noted that k values and valence populations of atoms belonging to the phosphate group agree with those found in KTiOPO₄ (Hansen, Protas & Marnier, 1991), where the total PO₄ charge was -1.85 (17). The values of charges in triphylite correspond closely to the electron density redistribution based on atomic electronegativities, but differ significantly from formal oxidation values. That is, they result from the partly covalent character of bonding in tetrahedral and octahedral triphylite sites. Nevertheless the net charges derived from multipole parameters should be interpreted cautiously because of their dependence on the type of monopole functions used.

Concluding remarks

Application of the multipole refinement technique to the study of the deformation density distribution in synthetic triphylite LiFePO₄ has brought significant model improvements in comparison with conventional all-data and high-order refinements and has allowed evaluation of the Fe d -orbital occupancies. Fairly consistent pictures of the deformation density distribution have been obtained in the sense that the observed features were similar to those in chemically equivalent groups of other crystals. An attempt was made to find a correlation between the features of the deformation density at room temperature and magnetic properties of LiFePO₄ below the Néel temperature. We note that a clearer picture of exchange interactions can be obtained from an electron spin density study.

We thank N. Bouhmaida and N. Ghermani (Nancy) for their help concerning the transformation of d -orbital populations. ELB and VGT would like to thank Professor V. S. Urusov and Dr O. V. Yakubovich for their collaboration in the previous crystallographic study of triphylite.

References

- ABRAHAMS, S. C. & KEVE, E. T. (1971). *Acta Cryst.* **A27**, 157-165.
 BECKER, P. & COPPENS, P. (1974). *Acta Cryst.* **A30**, 129-147.
 BELOV, N. V., IVASCHENKO, A. N. & MATVIENKO, E. N. (1981). *Mineral. J.* **3**, 56-66. (In Russian.)
 BLESSING, R. H. (1988). *Acta Cryst.* **B44**, 334-340.
 CLEMENTI, E. & RAIMONDI, D. L. (1963). *J. Chem. Phys.* **38**, 2686-2689.
 COPPENS, P., GURU ROW, T. N., LEUNG, P., STEVENS, E. D., BECKER, P. J. & YANG, Y. W. (1979). *Acta Cryst.* **A35**, 63-72.

- DRAPER, N. R. & SMITH, H. (1981). *Applied Regression Analysis*, 2nd ed. New York: Wiley.
- FUJINO, K., SASAKI, S., TAKEUCHI, Y. & SADANAGA, S. (1981). *Acta Cryst.* **B37**, 513–518.
- GERR, R. G., BOROVSKAYA, T. N., VOLOSHINA, I. V., LOBANOV, N. N., SLOVOKHOTOVA, O. L., STRELTSOV, V. A., STRUCHKOV, Y. T., OZEROV, R. P., TSIRELSON, V. G. & YANOVSKII, A. I. (1991). *J. Struct. Chem.* Submitted.
- HANSEN, N. K. (1991). In *Logiciels pour la Chimie – Catalogue de Logiciels de Recherche*, edited by La Société de Chimie Française, Paris.
- HANSEN, N. K. & COPPENS, P. (1978). *Acta Cryst.* **A34**, 909–921.
- HANSEN, N. K., PROTAS, J. & MARNIER, G. (1991). *Acta Cryst.* **B47**, 660–672.
- HOLLADAY, A., LEUNG, P. & COPPENS, P. (1983). *Acta Cryst.* **A39**, 377–387.
- JOHNSON, C. K. (1965). *ORTEP*. Report ORNL-3794. Oak Ridge National Laboratory, Tennessee, USA.
- KURKI-SUONIO, K. (1977). *Isr. J. Chem.* **16**, 115–123.
- LARSON, A. C. (1970). In *Crystallographic Computing*, edited by F. R. AHMED. Copenhagen: Munksgaard.
- SANTORO, R. P. & NEWNHAM, R. E. (1967). *Acta Cryst.* **22**, 344–347.
- STRELTSOV, V. A., TSIRELSON, V. G. & OZEROV, R. P. (1990). In *Problems of Crystal Chemistry*, edited by M. A. PORAI-KOSHITS. Moscow: Nauka. (In Russian.)
- TSIRELSON, V. G., STRELTSOV, V. A., OZEROV, R. P. & IVON, K. (1989). *Phys. Status Solidi A*, **115**, 515–521.
- YAKUBOVICH, O. V., BELOKONEVA, E. L., TSIRELSON, V. G. & URUSOV, V. S. (1990). *Vestnik Moscow Univ.* **4**, 99–105. (In Russian.)
- YAKUBOVICH, O. V., SIMONOV, M. A. & BELOV, N. V. (1977). *Sov. Phys. Dokl.* **22**, 347–348.

Acta Cryst. (1993). **B49**, 153–158

Maximum Entropy as a Tool for the Determination of the *c*-Axis Profile of Layered Compounds

BY PH. DEPONDY

Département de Recherches Physiques (URA CNRS 71), Université Pierre et Marie Curie, 75252 Paris CEDEX 05, France

D. A. NEUMANN

Reactor Radiation Division, National Institute of Standards and Technology, Gaithersburg, MD 20899, USA

AND S. F. TREVINO

ARDEC, Picatinney Arsenal, NJ, USA, and Reactor Radiation Division, National Institute of Standards and Technology, Gaithersburg, MD 20899, USA

(Received 15 June 1992; accepted 29 October 1992)

Abstract

A simple procedure for the determination of the structure normal to the basal plane of layered compounds based on the now ubiquitous maximum-entropy method is presented. It is illustrated by the analysis of room-temperature (00 l) elastic neutron-scattering experiments performed on two graphite intercalation compounds, stage 3 C_{44,6}MoCl₅ and stage 1 KC₂₄(ND₃)_{4,3}. The former example is quite simple, requiring only a crude heuristic model to determine the structure-factor phases. The latter shows good sensitivity to the orientation of the ND₃ threefold axis with respect to the basal plane, thus providing its first direct determination.

1. Introduction

The properties of many layered materials, such as graphite, transition-metal dichalcogenides and layer silicates, can be substantially altered by the inter-

calation of various guest species into the interlayer region (gallery) of the host. Because of the lack of single crystals and the prevalence of stacking faults, complete structural determinations of these systems are seldom made. However, owing to the 'platelike' nature of the individual pieces, it is often possible to fabricate oriented specimens in which the *c* axes (*i.e.* the direction perpendicular to the basal planes) of the pieces are well aligned, but the in-plane crystallographic axes are not. One can then use X-ray or neutron scattering to obtain scans along the *c* direction – (00 l) scans – which reflect important structural information in these materials, such as the distance between guest and host layers, the guest density within the galleries, the orientation of polyatomic guests and, for graphite intercalation compounds, the stage. Furthermore, because of the complicated phase diagrams of these materials, such information is required before any meaningful interpretation of other data can be made. Thus, one requires a method